Configurations of the N-Terminal Amphipathic Domain of the Membrane-Bound M13 Major Coat Protein†

Alexander B. Meijer, Ruud. B. Spruijt, Cor J. A. M. Wolfs, and Marcus A. Hemminga*

Department of Biomolecular Sciences, Laboratory of Biophysics, Wageningen University and Research Center, Dreijenlaan 3, 6703 HA Wageningen, The Netherlands

Received October 3, 2000; Revised Manuscript Received February 12, 2001

ABSTRACT: The M13 major coat protein has been extensively studied in detergent-based and phospholipid model systems to elucidate its structure. This resulted in an L-shaped model structure of the protein in membranes. An amphipathic α-helical N-terminal arm, which is parallel to the surface of the membrane, is connected via a flexible linker to an α-helical transmembrane domain. In the present study, a fluorescence polarity probe or ESR spin probe is attached to the SH group of a series of N-terminal single cysteine mutants, which were reconstituted into DOPC model membranes. With ESR spectroscopy, we measured the local mobility of N-terminal positions of the protein in the membrane. This is supplemented with relative depth measurements at these positions by fluorescence spectroscopy via the wavelength of maximum emission and fluorescence quenching. Results show the existence of at least two possible configurations of the M13 amphipathic N-terminal arm on the ESR time scale. The arm is bound either to the membrane surface or in the water phase. The removal or addition of a hydrophobic membrane-anchor by site-specific mutagenisis changes the ratio between the membrane-bound and the water phase fraction.

The M13 major coat protein of the filamentous bacteriophage M13 is studied to elucidate fundamental questions involving protein−DNA, protein−lipid, and protein−protein interactions. With about 2800 copies, the M13 major coat protein is most abundant protein in the phage, where it protects the single stranded viral DNA (for a review, see ref *1*). During the infection of the *Escherichia coli* cell, newly synthesized protein is stored into the inner membrane before it is used in the production of new bacteriophages (*2*). For understanding, the mechanisms involved in the viral reproduction cycle, knowledge is essential about the membrane-bound assembly and dynamics of the M13 coat protein.

The primary structure of the coat protein consists of 50 amino acids (Figure 1) in which three domains can be distinguished: an acidic amphipathic N-terminal arm, a hydrophobic segment, and a basic C-terminus (*3*, *4*). The protein has been extensively studied in membrane-model systems by biophysical techniques. These studies resulted in an L-shaped structure of the protein in a membrane (*5*−*7*). In this model, an amphipathic N-terminal helix is oriented parallel to the surface of the membrane and is connected with a flexible linker to a transmembrane α-helix. The assignments of amino acids in the helical domains are schematically depicted in Figure 1. The N-terminal segment of SDS-bound M13 coat protein showed dynamics on the picosecond and nanosecond time scale as was shown by NMR spectroscopy (*8*, *9*).

Relative depth and local dynamics of specific sites in the protein, reconstituted in phospholipid model membranes, were measured by a single cysteine-scanning approach. In this approach, a fluorescence or ESR probe was attached to specific sites in the M13 major coat protein (*10*−*12*). Fluorescence quenching, magnetization quenching, mobility, and polarity probing showed a surprisingly deep burial of the C-terminal lysine residues in the membrane. In contrast, the two phenylalanines are in a more shallow position. The organization of those amino acids are suggested to comprise an anchor of the C-terminal end to the membrane (*10*, *11*). Furthermore, a fluorescence study showed the importance of leucine 14 and phenylalanine 11 for the anchoring interactions of the amphipathic N-terminal arm to the membrane. Replacement of those amino acids residues by alanines resulted in a more extended configuration of the N-terminal arm (*12*).

Site-specific spin labeling has been employed for a number of membrane and soluble proteins to obtain structural information (*13*, *14*). The dynamics of nitroxide spin labels are significantly affected by the local structure and environment of the position to which they are attached to the M13 protein (*11*). In the present study, additional information is obtained about the N-terminal section of the protein, reconstituted in DOPC,[1] by using ESR and fluorescence spectroscopy. Our results indicate the presence of a membrane-bound and a more extended configuration of the N-terminal section of the protein.

† This research was supported by the Life Sciences Foundation (SLW) with financial aid of The Netherlands Organization for Scientific Research (NWO).

* To whom correspondence should be addressed. Phone: 31-317482044. Fax: 31-317-482725. E-mail: marcus.hemminga@virus.mf.wau.nl.

[1] Abbreviations: IAEDANS, *N*-(iodoacetyl)aminoethyl-1-sulfonaphthylamine; DOPC, dioleoylphosphatidylcholine; *L*/*P*, lipid to protein molar ratio; SDS, sodium dodecyl sulfate; λ_{max}, wavelength of maximum emission; K_{sv}, Stern−Volmer constant; WT coat protein, wild-type major coat protein.

10.1021/bi002306o CCC: $20.00
Published on Web 03/29/2001

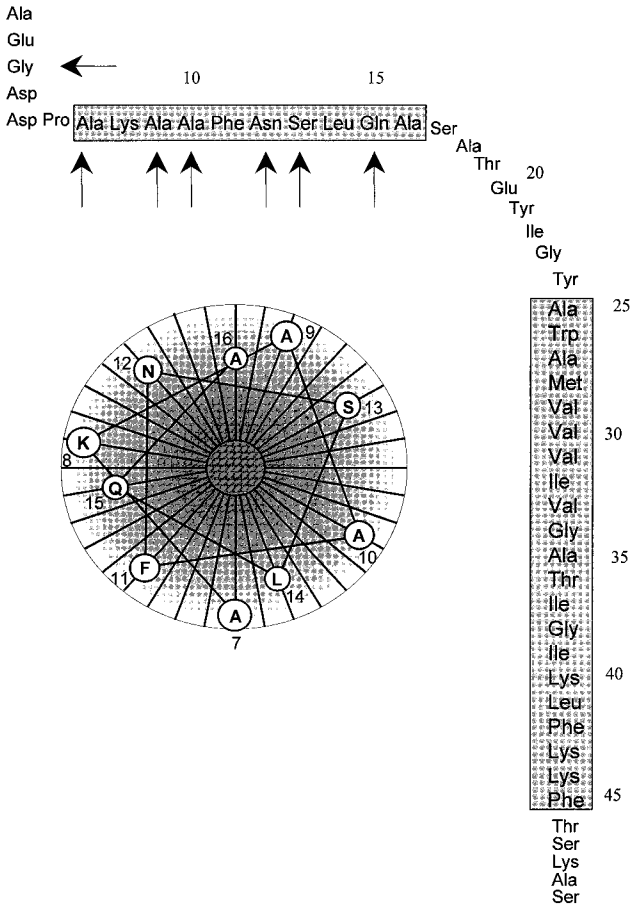

FIGURE 1: Arbitrary representation of the primary structure of the M13 major coat protein (*3*). The arrows point to the positions that are mutated into cysteine residues. The boxed regions represents the amphipathic and transmembrane helix (*9*, *26*). The inset shows amino acids 7−16 in an α-helix.

MATERIALS AND METHODS

Preparation and Purification of Labeled Single Cysteine Mutants. Site-specific cysteine mutants were prepared with the QuikChange Site-Directed Mutagenisis Kit from Stratagene. The vector pT7-7, with the major coat protein geneVIII as insert was used as the template for this procedure. The oligo-nucleotides were purchased from Amersham Pharmacia Biotech. The sequence of the mutant DNA was verified using automated DNA sequencing. Correctly mutated plasmid DNA was transformed into competent *E. coli* BL21(DE3) cells (*15*).

Mutant M13 coat protein was purified, and labeled with IAEDANS as is described by Spruijt et al. (*12*). First was mutant protein overexpressed in *E. coli*, and the membrane fraction was collected. Second, the membrane proteins were extracted from the membrane, and separated on hydrophobicity using reversed-phase chromatography. After this step, the about 85% pure mutant coat protein was in a mixture of 35% 2-propanol/water (v/v) and 0.1% triethylamine (v/v). The mutant coat protein was subsequently labeled with IAEDANS (Molecular Probes) or maleimido-proxyl (Sigma). Slight modifications were introduced in the procedure for the attachment of 3-maleimido-proxyl spin label to the single cysteine mutants. An excess of spin-label was added to the protein fraction after reversed-phase chromatography. The label was allowed to react with the SH-groups of the mutants for 30 min at 20 °C. The labeling reaction was stopped by an addition of an excess of β-mercaptoethanol. In the final step, free label and remaining impurities were removed from the labeled mutant coat proteins using size exclusion chromatography. The about 95% pure protein, labeled with IAEDANS or maleimido-proxyl, was now in a buffer containing 50 mM cholate, 10 mM Tris-HCl, 1 mM EDTA, 150 mM NaCl at pH 8.

Reconstitution of Labeled M13 Coat Protein. Labeled M13 major coat protein was reconstituted into DOPC (Avanti polar lipids) using the cholate-dialysis method (*16*). The amount of protein was chosen such that the lipid-to-protein molar ratio (*L*/*P*) was about 100. Samples contained about 4 mg of phospholipids for ESR spectroscopy and about 1 mg for fluorescence spectroscopy. Chloroform was evaporated from the desired amount of phospholipid solution and the residual traces of chloroform were removed by drying under vacuum for at least 2 h. The lipids were subsequently solubilized in 50 mM cholate, 1 mM EDTA, 150 mM NaCl, 10 mM Tris-HCl, pH 8, and mixed with labeled protein. In the following step, the lipid−protein mixture was dialyzed for 60 h against a 100-fold excess buffer containing 1 mM EDTA, 150 mM NaCl, 10 mM Tris-HCl at pH 8. The buffer was replaced every 12 h.

Steady-State Fluorescence Spectroscopy. Fluorescence spectra of the labeled mutants were collected at 22 ± 0.5 °C using an excitation wavelength of 340 nm on a SPEX Fluorolog 3-22 fluorometer equipped with a 450 W xenon lamp as an excitation source. Excitation and emission bandwidths were set to 1 and 3 nm, and spectra were recorded between 400 and 600 nm. Samples of 1 mL were in 1 cm light-path fused silica cuvettes (Hellma model 114F-QS), and the optical density at 340 nm never exceeded 0.1. The spectra were corrected for background signal (empty vesicles) and sensitivity of the photomultiplier. The wavelength of maximum emission (λ_{max}) was obtained from the fluorescence data.

Fluorescence quenching data were obtained and analyzed as described by Meijer et al. (*17*). Aliquots of an acrylamide stock solution (3 M acrylamide, 150 mM NaCl, 10 mM Tris-HCl, 1 mM EDTA, pH 8) were added to samples of labeled protein that was reconstituted into in DOPC. After every addition of acrylamide, the decrease in fluorescence intensity was measured. Appropriate corrections for dilution were made for these quenching experiment. The Stern−Volmer constant (K_{sv}) was obtained from the fluorescence data (*18*, *19*) according to the Stern−Volmer equation for collisional quenching:

$$\frac{F_o}{F} = 1 + K_{sv}[Q]$$

where F_o and F are the fluorescence intensities in the absence and the presence of the quencher Q. K_{sv} is the Stern−Volmer quenching constant.

ESR Spectroscopy. A comparable experimental set up was used as is described in Stopar et al. (*20*). Samples of 1 mL of reconstituted mutant coat protein were freeze-dried overnight, and dissolved in 10 mM Tris-HCl, 1 mM EDTA, and 150 mM NaCl, pH 8, yielding multilamellar vesicles. The vesicles were concentrated by centrifugation at 20 000

rpm in a Beckman Ti75 rotor at 20 °C. Fifty microliter glass capillaries were filled up to 5 mm with vesicles containing labeled mutant coat protein. These capillaries were inserted into standard 4 mm diameter quartz tubes. ESR spectra were recorded on a Bruker ESP 300E ESR spectrometer equipped with a 108TMH/9103-microwave cavity. The temperature was regulated with a nitrogen gas-flow-temperature system. The ESR settings for all recorded spectra were 6.38 mW, microwave power; 0.1 mT, modulation amplitude; 40 ms, time constant; 160 s, scan time; 10 mT, scan width; and 342.0 mT, center field. Up to 20 recorded spectra were accumulated.

Stopar et al. (*20*) calculated the rotational correlation time τ_c for the labeled A49C and S30C mutants according to Marsh et al. (*21*). The same approach was used to calculate the rotational correlation time of mobile single component spectra (10^{-11} s $\leq \tau_c \leq 3 \times 10^{-9}$ s). It is not possible to characterize the rotational mobility of the mobile component in spectra which display two spectral components. Especially, the center line width is distorted because of the overlap of the spectral components. However, τ_c was estimated using the line width of the high field line. For this purpose, the single component spectrum of the A7C/L14A mutant was recorded at various temperatures, and τ_c was subsequently calculated according to Marsh et al. (*21*). By plotting the line width vs τ_c, a reference is acquired for the corresponding τ_c in the mixed spectra.

To determine the amount of nonspecific labeling of mutant coat protein with 3-maleimido-proxyl, the purification and labeling procedure was repeated for the wild-type coat protein. Labeled wild-type protein was reconstituted into DOPC and the ESR spectrum was recorded. The result showed the presence of a small amount (about 5%) of nonspecific labeling for all mutant coat proteins.

RESULTS

The ESR spectra of the A7C, A7C/A10I, Q15C, Q15C/L14A, and Q15C/A10I mutants (in DOPC) displayed a superposition of two components at 20 °C. The resolution between both components was enhanced at lower temperatures, therefore, the spectra were acquired at 5 °C. The spectra consisted of a sharp three-line spectrum representing mobile probes on the ESR time-scale (10^{-11} s $\leq \tau_c \leq 3 \times 10^{-9}$ s), and a broad spectral component indicative for motion in the slow regime ($\tau_c \geq 2 \times 10^{-9}$ s) (*21*). On the other hand, the spectrum of the A7C/L14A mutant only consisted of a mobile component. Figure 2 shows the spectra of the A7C, A7C/L14A, A7C/A10I, Q15C/L14A, Q15C, and Q15C/A10I mutants. An estimate of the immobile fraction was acquired in a subtraction procedure by using the spectrum of the A7C/L14A mutants as a reference. Table 1 shows the estimated fractions of immobile component per mutant.

Spruijt et al. (*12*) labeled the A7C, A7C/L14A, and A7C/A10I with IAEDANS, and the mutants were reconstituted into DOPC/DOPG (4:1 molar ratio) to obtain the relative depth of the probe in the membrane. In the present study, this approach was repeated for the Q15C, Q15C/L14A, and Q15C/A10I mutants, which were reconstituted into DOPC for optimal comparison with the ESR spectra. The fluorescence data of the Q15C, Q15C/L14A, and Q15C/A10I are shown in Table 1. This table also shows the results from the fluorescence study by Spruijt et al. (*12*).

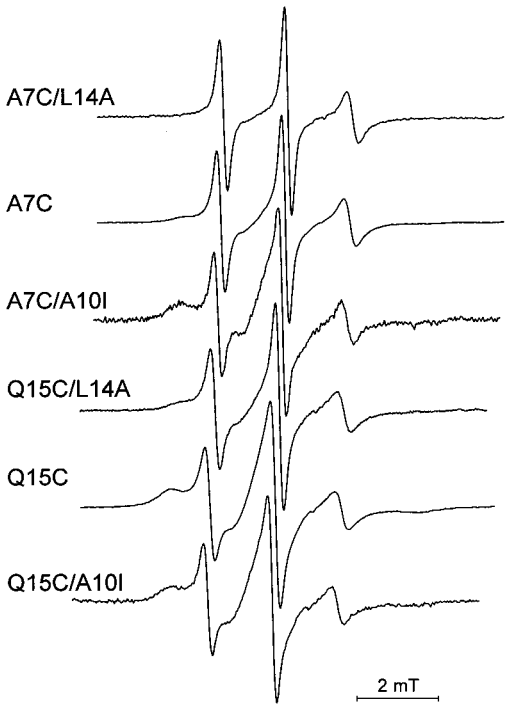

FIGURE 2: ESR spectra of the 3-maleimido proxyl site-specific labeled A7C/L14A, A7C, A7C/A10I, Q15C/L14A, Q15C, and Q15C/A10I mutants, which were reconstituted into DOPC multilamellar vesicles at *L*/*P* 100 in 150 mM NaCl, 10 mM Tris-HCl,1 mM EDTA, pH 8 at 5 °C. The central spectral line-heights are normalized to each other.

Table 1: Environmental Polarity and Stern−Volmer Quenching Constant of A7C-Derived Mutants in DOPC/DOPG (4/1 molar ratio) and Q15C-Derived Mutants in DOPC, and the Fraction Immobile ESR Spectral Component of the A7C and Q15C-Derived Mutants in DOPC

mutant	λ_{max}	K_{sv} (M^{-1})	estimated fraction immobile component in the ESR spectrum (%)
A7C	495[a]	3.0[a]	33
A7C/L14A	502[a]	5.4[a]	0
A7C/A10I	492[a]	2.6[a]	75
Q15C	492	1.2	77
Q15C/L14A	497	1.9	53
Q15C/A10I	491	0.9	80

[a] Wavelengths of maximum emission (λ_{max}) and Stern−Volmer constant (K_{sv}) were measured by Spruijt et al. (*12*) on AEDANS labeled A7C-derived mutant coat proteins, which were reconstituted into DOPC/DOPG (4/1 molar ratio) at an L/P of 100. Acrylamide was used as a fluorescence quencher.

ESR spectra of the seven labeled single-cysteine mutants (indicated in Figure 1) were recorded to study the properties of the N-terminus of the M13 major coat protein. Except from the G3C spectrum, the spectra clearly show two spectral components. Figure 3 shows the spectra of the G3C, A9C, A10C, N12C, and S13C mutants reconstituted into DOPC at 5 °C. The fraction of immobile component was again estimated from the spectra (Figure 4). Only a small fraction of the G3C mutant spectrum consisted of immobile component; therefore, the immobile fraction was set to zero percent. A rotational correlation time τ_c was calculated from the single component spectra of the A7C/L14A and G3C

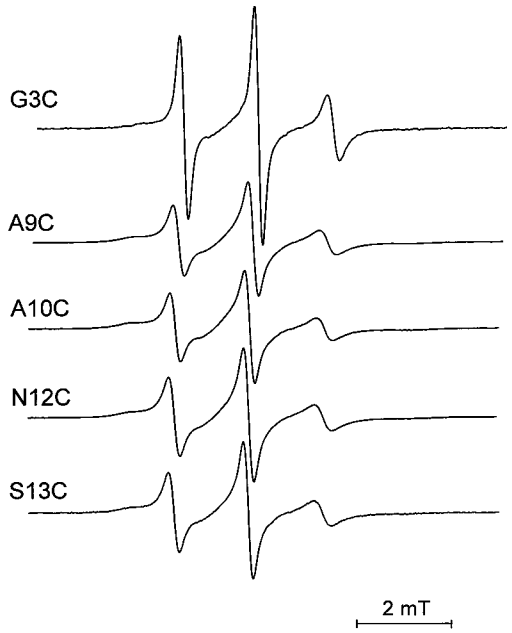

FIGURE 3: ESR spectra of the 3-maleimido proxyl site-specific labeled G3C, A9C, A10C, N12C, and S13C mutants, which were reconstituted into DOPC multilamellar vesicles at *L*/*P* 100 in 150 mM NaCl, 10 mM Tris-HCl, 1 mM EDTA, pH 8 at 5 °C. The spectra are normalized to one in the double intregral.

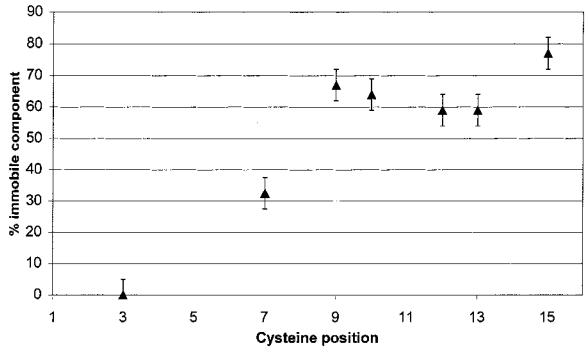

FIGURE 4: Estimated fraction of immobile component from the ESR spectra of 3-maleimido proxyl site-specific spin-labeled mutant coat proteins at various positions. The labeled proteins were reconstituted in DOPC multilamellar vesicles at *L*/*P* 100 in 150 mM NaCl, 10 mM Tris-HCl, 1 mM EDTA, pH 8 at 5 °C. The A7C/L14A spectrum was used as a reference in the spectral subtraction procedure.

mutants. This resulted in a τ_c of about 1.1 ns. The estimated rotational correlation time of the mobile components in the mixed spectra was about 1.4 ns for the A7C mutant, and about 1.7 ns for the mutants with a cysteine at the positions 9, 10, 12, 13, and 15. The outer hyperfine splitting $2A_{zz}$ of the immobile component was between 5.9 and 6.0 mT in the mixed spectra of the mutant coat proteins.

DISCUSSION

With the cysteine scanning approach, information can be obtained at specific sites in the reconstituted M13 coat protein (*10*−*12*, *20*). The relative depth of sites in the membrane was assessed by attaching the fluorescence polarity probe IAEDANS to mutant proteins. The depth was subsequently determined via the wavelength of maximum emission (λ_{max}), because probes have a more red-shifted λ_{max} outside than inside the membrane (*10*, *12*, *17*, *22*). This was further substantiated by using fluorescence quenchers that predominantly affect probes inside (5-SASL) or outside (acrylamide) the membrane.

By using the above-mentioned approach, Spruijt et al. (*12*) showed the importance of phenylalanine 11 and leucine 14 for the anchoring interactions of the amphipathic N-terminal arm to the surface of a DOPC/DOPG (4/1 molar ratio) model membrane. After replacement of leucine 14 by an alanine, the monitored position 7 moved toward the water phase. On the other hand, the replacement of alanine 10 for an isoleucine resulted in a deeper burial of position 7 into the membrane.

In the present study, the N-terminal arm is studied with spin label ESR spectroscopy. The spin probe 3-maleimido-proxyl, which is used in this study, is smaller in size than the IAEDANS probe, and mainly provides information about the local dynamics of the site to which the probes is attached. Surprisingly, the ESR data of the 3-maleimido-proxyl labeled position 7 shows the presence of two species of motion on the ESR time scale, represented by broad and a sharp spectral component. The sharp component exhibited an isotropic hyperfine splitting of about 1.6 mT. Earlier studies with 3-maleimido-proxyl, and related nitroxide probes have shown that this is an indication for an hydrophilic environment (*20*, *23*).

The replacement of hydrophobic leucine 14 by alanine, which decreases the anchoring capacity of the N-terminus to the surface of the membrane, results in the disappearance of the broad component in the spectrum of the A7C/L14A mutant. As compared to the mobile component in the spectrum of A7C mutant, the rotational correlation time slightly decreases in the spectrum of the A7C/L14A mutant. This suggests a higher segmental motion at this position. This change in mobility cannot be caused by a dramatic change in secondary structure, because no conformational change was detected with CD spectroscopy in the L14A and A10I mutant coat proteins (*12*). The mutation of an alanine 10 to an isoleucine, which increases the anchoring capacity of the N-terminal arm to the surface of the membrane, results in a higher fraction of immobile component. This components increases with about 42% upon comparing the spectra of the A7C and A7C/A10I mutant (see Table 1). The combination of the fluorescence and ESR results strongly suggests that the mobile component represents a position in the water phase and the immobile component a membrane-bound fraction of the protein.

The replacement of leucine 14 by alanine has an effect throughout the N-terminal section of the protein as is demonstrated with the Q15C and Q15C/L14A mutants. The λ_{max} of AEDANS is red shifted by 5 nm as a result of the mutation which suggests a more polar environment for position 15. This is in agreement with the finding that the probe is also more easily quenched by acrylamide, as is demonstrated by the higher Stern−Volmer constant (Table 1). Finally, the ESR data show a decrease of 24% in the fraction of immobile component in the Q15C/L14A mutant as compared to the ESR data of the Q15C mutant. These results show that the monitored position 15 shifts toward the water phase when the hydrophobic "membrane-anchor" leucine 14 is replaced by an alanine.

However, the immobile component does not completely disappear as is the case in the spectrum of the A7C/L14A mutant. In other words, about 53% of the N-terminal arms remain bound to the surface of the membrane in the Q15C/L14A mutant on the ESR time scale (Table 1). This shows that the N-terminus does not entirely shifts to the water phase as a result of the removal of leucine 14. Position 15 in the Q15C/A10I mutant is hardly sensitive to the addition of the hydrophobic amino acid isoleucine at position 10. The ESR spectrum of the Q15C/A10I mutant showed only a small increase of about 3% in the fraction of immobile component as compared to the Q15C mutant. Such a small effect is also seen in the fluorescence results (Table 1). This apparent insensitivity to the additional "anchoring" amino acid isoleucine (with position 7 being highly sensitive) shows that position 15 is close to a hinge point when the N-terminal arm is more tightly bound to the surface of the membrane.

The ESR data of the measured positions in the N-terminal section of the protein clearly show the presence of two fractions at every position (Figure 3). The positions 9−13 show an approximate equal membrane-bound fraction of about 65%. Position 7 displays a smaller membrane-bound fraction of 30%. This is not a surprise, since it is close to the unstructured (acidic) end of the protein, which is probably most of the time in the water phase. On the contrary, position 15 exhibits a higher percentage (77%) of membrane-bound fraction. Fluorescence quenching results by Spruijt et al. (*12*) showed that position 15 is buried deeper into the membrane as compared to the other N-terminal positions. It should be noted that the amino acid residues 17−24 between the amphipathic N-terminal arm and the transmembrane helix are even deeper buried in the membrane (*12*). This can explain the higher membrane-bound fraction in the spectrum of position 15.

Information about local dynamics at the labeled positions can be obtained from the spectral components in the spectra. The motion of the spin probe attached to the protein will be determined by the local environment as well as the local conformation of the protein. The hyperfine splitting $2A_{zz}$ of 5.9−6.0 mT of the broad membrane-bound component in the ESR spectra is less than the rigid limit nitroxide spectrum (∼7.0 mT). Probably, the spin label 3-maleimido-proxyl exhibits a wobbling motion in a cone at the cysteine residue as was suggested in earlier studies with 3-maleimido-proxyl labeled protein (*20*, *24*, *25*). The membrane-bound components in the spectra do not reveal much details about the local mobility. However, it is conceivable that the probes in this membrane-bound fraction represent the N-terminal amphipathic helix in the L-shaped model of the protein. One would expect that probes at positions facing the water phase side of the helix exhibit a higher mobility than do probes facing the membrane side of the helix. Indeed, $2A_{zz}$ of the positions 9, 12, and 13 are smaller than $2A_{zz}$ of the positions 7, 10, and 15 (5.9 vs 60 mT). However, these differences in $2A_{zz}$ are too small to draw reliable conclusions about changes in the probe mobility of the membrane-bound fractions. The mobility of the spin-probes is apparently mainly affected by the local structure of the N-terminal helix.

The line width of the mobile components from the single cysteine mutant spectra result in a rotational correlation time (τ_c) between 1.1 and 1.7 ns. Apparently, there is a higher backbone mobility in the water-phase fraction as compared to the membrane bound fraction of the N-terminal arm of the protein. Interestingly, the measured rotational correlation times of the water-phase fraction correspond to a motional freedom in the nanosecond time scale, similar as found for the N-terminal part of SDS-dissolved M13 coat protein with NMR spectroscopy (*8*, *9*). The local conformation of the N-terminal arm probably unfolds when the N-terminal arm is relocated to the water phase, which subsequently produces the higher backbone mobility. The relocation of the N-terminal arm from the water phase to the surface of the membrane, and subsequent refolding into the amphipathic helix is sufficiently slow (on the ESR time scale) to detect two clearly resolved spectral components.

CONCLUSION

With a cysteine scanning approach, information about dynamics and penetration depth in a phospholipid model membrane can be acquired of specific sites in the protein. The amphipathic N-terminal section of the M13 major coat protein exists in at least two possible configurations. One fraction of the protein has its N-terminal arm in the water phase. In the other fraction, the N-terminus is bound to the surface of the membrane. The water phase component shows high segmental (backbone) mobility. On the contrary, the membrane-bound N-terminus is much slower in motion, and probably represents the "L-shaped" structure of the protein. The ratio between both fractions can be modified by the addition or removal of an hydrophobic "membrane-anchor".

REFERENCES

1. Marvin, D. A. (1998) *Curr. Opin. Struct. Biol. 8*, 150−158.
2. Mandel, G., and Wickner, W. (1979) *Proc. Natl. Acad. Sci. U.S.A. 76*, 236−240.
3. Van Wezenbeek, P. M. G. F., Hulsebos, T. J. M., and Schoenmakers, J. G. G. (1980) *Gene 11*, 129−148.
4. Marvin, D. A., Hale, R. D., Nave, C., and Citterich, M. H. (1994) *J. Mol. Biol. 235*, 260−286.
5. McDonnell, P. A., Shon, K., Kim, Y., and Opella, S. J. (1993) *J. Mol. Biol. 233*, 447−463.
6. Wolkers, W. F., Spruijt, R. B., Kaan, A., Konings, R. N. H., and Hemminga, M. A. (1997) *Biochim. Biophys. Acta 1327*, 5−16.
7. Marassi, F. M., Ramamoorthy, A., and Opella, S. J. (1997) *Proc. Natl. Acad. Sci. U.S.A. 94*, 8551−8556.
8. Papavoine, C. H. M., Remerowski, M. L., Horstink, L. M., Konings, R. N. H., Hilbers, C. W., and van de Ven, F. J. M. (1997) *Biochemistry 36*, 4015−4026.
9. Almeida, F. C. L., and Opella, S. J. (1997) *J. Mol. Biol. 270*, 481−495.
10. Spruijt, R. B., Wolfs, C. J. A. M., Verver, J. W. G., and Hemminga, M. A. (1996) *Biochemistry 35*, 10383−10391.
11. Stopar, D., Jansen, K. A. J., Pali, T., Marsh, D., and Hemminga, M. A. (1997) *Biochemistry 36*, 8261−8268.
12. Spruijt, R. B., Meijer, A. B., Wolfs, C. J. A. M., and Hemminga, M. A. (2000) *Biochim. Biophys. Acta 1509, 311−323*
13. Hubbell, W. L., and Altenbach, C. (1994) *Curr. Opin. Struct. Biol. 4*, 566−573.
14. Hubbell, W. L., Gross, A., Langen, R., and Lietzow, M. A. (1998) *Curr. Opin. Struct. Biol. 8*, 649−656.
15. Studier, F. W., Rosenberg, A. H., Dunn, J. J., and Dubendorf, J. W. (1990) *Methods Enzymol. 185*, 60−89.
16. Spruijt, R. B., Wolfs, C. J. A. M., and Hemminga, M. A. (1989) *Biochemistry 28*, 9158−9165.

17. Meijer, A. B., Spruijt, R. B., Wolfs, C., and Hemminga, M. A. (2000) *Biochemistry 39*, 6157−6163.
18. Lehrer, S. S., and Leavis, P. C. (1978) *Methods Enzymol. 49*, 222−236.
19. Lehrer, S., S. (1971) *Biochemistry 10*, 3254−3263.
20. Stopar, D., Spruijt, R. B., Wolfs, C. J. A. M., and Hemminga, M. A. (1996) *Biochemistry 35*, 15467−15473.
21. Marsh, D. (1981) in *Membrane Spectroscopy* (Grell, E., Ed.) pp 51−142, Springer-Verlag, New York.
22. Hudson, E. N., and Weber, G. (1973) *Biochemistry 12*, 4154−4161.
23. Fretten, P., Morris, S. J., Watts, A., and Marsh, D. (1980) *Biochim. Biophys. Acta 598*, 247−259.
24. Vriend, G., Schilthuis, J. G., Verduin, B. J. M., and Hemminga, M. A. (1984) *J. Magn. Reson. 58*, 421−7.
25. Hemminga, M. A., and Faber, A. J. (1986) *J. Magn. Reson. 66*, 1−8.
26. Papavoine, C. H. M., Christiaans, B. E. C., Folmer, R. H. A., Konings, R. N. H., and Hilbers, C. W. (1998) *J. Mol. Biol. 282*, 401−419.

BI002306O